Morawska, P. O. et al. (2015) Side-chain influence on the mass density and refractive index of polyfluorenes and star-shaped oligofluorene truxenes. *Journal of Physical Chemistry C*, 119(38), pp. 22102-22107.

This is the author accepted manuscript.

There may be differences between this version and the published version. You are advised to consult the publishers' version if you wish to cite from it.

The published version is available:
doi:10.1021/acs.jpcc.5b05526)

http://eprints.gla.ac.uk/159767/

Deposited on: 29 March 2018

Side chain influence on the mass density and refractive index of polyfluorenes and star-shaped oligofluorene truxenes

Paulina O. Morawska[1], Yue Wang[1†], Arvydas Ruseckas[1], Clara Orofino-Peña[2], Alexander L. Kanibolotsky[2], Ramkumar Santhanagopal[3], Nils Fröhlich[3], Martin Fritsch[3], Sybille Allard[3], Ullrich Scherf[3], Peter J. Skabara[2], Ifor. D.W. Samuel[1], Graham A. Turnbull[1]

1. Organic Semiconductor Centre, SUPA, School of Physics and Astronomy, University of St Andrews, North Haugh, St Andrews KY16 9SS (UK)

2. WestCHEM, Department of Pure and Applied Chemistry, University of Strathclyde, 295 Cathedral Street, Glasgow G1 1XL, UK

3. Chemistry Department and Institute for Polymer Technology, Wuppertal University, Gauss-Str. 20, D-42119 Wuppertal, Germany

Abstract

The density of organic semiconductor films is an important quantity because it is related to intermolecular spacing which in turn determines the electronic and photophysical properties. We report on thin film density and refractive index measurements for polyfluorenes and star-shaped oligofluorene truxene molecules. An ellipsometer and a procedure using a spectrophotometer were used to determine film thickness and mass of spin-coated films, respectively. We present a study of the effect of alkyl side chains on the volumetric mass density and refractive index of the materials studied. The density measured for poly(9,9-di-n-octylfluorene) (PF8) was 0.88 ± 0.04 g/cm^3 and decreased with longer alkyl side chains. For

the truxene furnished with n-butyl groups (T3 butyl), we obtained a density of 0.90 ± 0.04 g/cm^3, which also decreased with increasing side-chain length.

Introduction

Thin films of organic semiconductors are used in a wide range of optoelectronic applications including photovoltaic devices [1,2], OLEDs [3,4], transistors [5], distributed feedback lasers [6,7,8], biological and chemical sensors [9,10,11]. Devices based on thin films are deposited by sublimation or from solution. The properties of materials in the solid-state depend not only on the electronic properties of individual molecules but also on how closely they pack together [12]. For instance, porphyrin-cored conjugated dendrimers showed dependence of the photoluminescence quantum yield (PLQY) on core − core interactions with various rings attached [13]. Charge transport also depends strongly on the intermolecular spacing as charges have to hop between molecules. The hopping process is strongly dependent on the intermolecular overlap of neighbouring molecules, and so also on the packing of the molecules [14,15]. Additionally, the spacing of molecules affects other important processes including exciton diffusion involved in highly efficient photovoltaic devices [16].

There is growing interest in measuring the microscopic morphology of the film using X-ray diffraction, atomic force microscopy, neutron scattering, and scanning electron microscopy but there are surprisingly few published measurements of film density. Methods reported in the literature used to study density of thin films include: the pressure-of-flotation method [17], X-ray reflectivity [18], selected-area electron diffraction combined with X-ray diffraction [19], and solution absorbance method [20]. In the pressure-of-flotation method the density is obtained by measuring the relative density difference and mass difference between a clean substrate

and a substrate with the deposited film. The relative density difference is found by applying pressure to a working liquid in which the test sample is placed, until the density of the liquid is in equilibrium with the density of the test sample. This method requires complex and sensitive apparatus to measure density values. The XRR and XRD methods analyse the reflected or diffracted beam from a very thin sample as a function of the angle of incidence and the angle of the detector. These methods can be used for density measurements of materials possessing crystalline structure but not in amorphous film. In the solution absorbance technique [20] the thickness of thin evaporated molecular film is measured with a surface profilometer and then the film is dissolved in a solvent. The absorbance of the resulting solution is compared against standards of the same material to determine the mass. The method is simple but has some limitations in its application to soft materials such as solution processed conjugated polymers since the surface profilometer can be inaccurate or even damage very thin polymer films.

In this paper we present density measurements of two families of fluorene-based organic semiconductors: long chain polyfluorenes and star-shaped oligodialkylfluorene truxenes. Polyfluorenes are well established printable OLED materials, while star-shaped analogues have been reported as low threshold, tuneable laser materials [21,22,23,24]. To measure the density of the spin-coated films we used an improved solution absorbance method. In this improved method we first removed the edge bead from the spin-coated films to give samples of uniform thickness and for higher accuracy used spectroscopic ellipsometry to measure thickness with higher accuracy. We investigated the effect of alkyl side chain length on the volumetric mass density and refractive indices for both fluorene families as well.

Experimental

The chemical structures of the polyfluorenes (PF) and oligofluorene truxenes (T3) studied in this paper are shown in Figure 1. The polyfluorene repeat units have either dioctyl (PF8), didodecyl (PF12) or dipentadecyl (PF15) alkyl side chains attached to the methylene bridge, these polymers being synthesied according to the procedures in references [25-28]. The star-shaped T3 molecules consist of a central truxene core with three terfluorene arms attached. Both the core and arms contain either butyl (T3 butyl) , hexyl (T3 hexyl) or octyl (T3 octyl) side chain substituents. The general synthesis of the T3 molecules can be found in reference [23]. The molecular weights of the truxene molecules and of the polymer repeat units are presented in table 1.

Material	Molecular weight of molecules or repeat unit of polymer [g/mol]
T3 butyl	3167
T3 hexyl	3840
T3 octyl	4513
PF8	389
PF12	501
PF15	585

Table 1. Molecular weights of the truxenes molecules and of the polymer repeat units

Absorption spectra were measured with a Cary 300 UV-Vis spectrophotometer. Fluorescence spectra were measured with a Jobin Yvon FluoroMax2. Values of absolute photoluminescence quantum yield (PLQY) of approximately 50 nm thick films were

measured using an integrating sphere [29] in a Hamamatsu Photonics C9920-02 system with continuous excitation at 355 nm by a monochromated Xenon lamp.
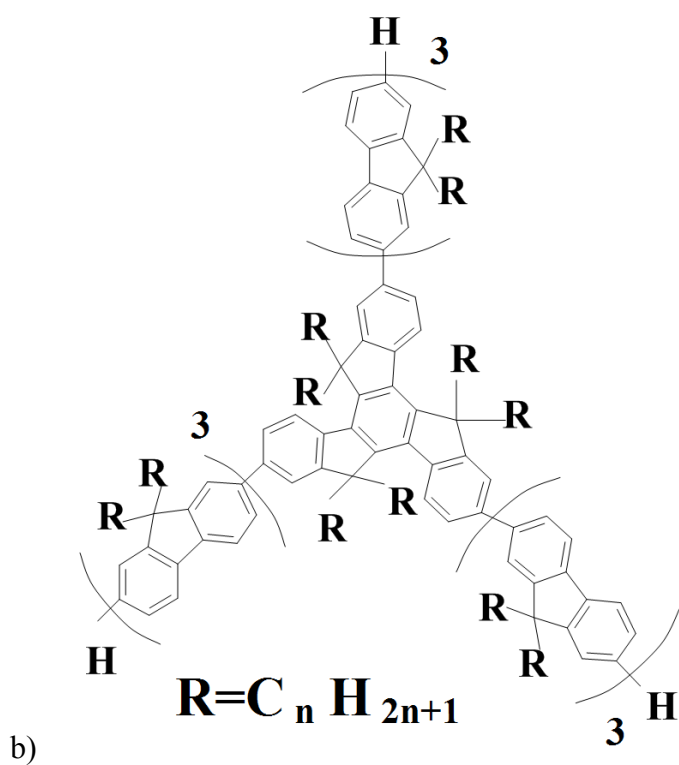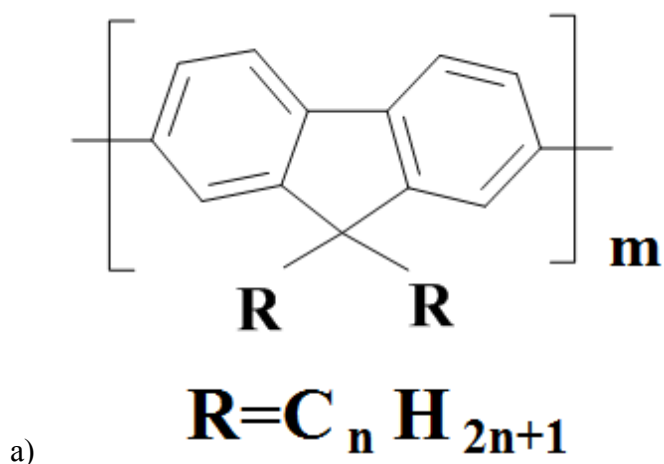

a)

$R = C_n H_{2n+1}$

b)

$R = C_n H_{2n+1}$

Figure 1. Chemical structure of a) polyfluorene (n = 8, 12, 15); b) tris(terfluorenyl)truxene (n = 4, 6, 8)

Samples for the density measurements were prepared on 15 mm × 15 mm silicon substrates. These were first cleaned by ultrasonification in acetone and isopropanol solvents for 10 min

each. Next, the substrates were treated in an oxygen plasma asher for 3 min. Films were deposited by spin-coating from chlorobenzene (for polyfluorenes) and toluene (for truxenes) solutions on the pre-prepared silicon wafers. The solution concentrations used were 15 mg/ml for PF8 and PF12, 7.5 mg/ml for PF15, and 12 mg/ml for all the truxene materials. For each material we fabricated four samples. To ensure that the films used in the experiment were of a uniform thickness across the whole substrate, a square section of area 10 mm × 10 mm was cleaved from the centre of a bigger substrate. The dimension of each cleaved substrate was accurately measured with calipers. The area of each piece of silicon wafer was measured by averaging five measurements of x and y substrate sides. The film thickness and refractive index were then measured by variable angle spectroscopic ellipsometry (J.A. Woollam Co. Inc. M2000-DI). This contactless measurement is based on determining changes in the polarization state of light reflected from the thin film. The spectroscopic range of the collected data was 190 nm – 1700 nm and the measurements were performed for incidence angles 45° – 75° in steps of 5°. To evaluate film thickness from the recorded data, a Cauchy model was fitted in the transparent range (between 480 nm – 1700 nm) for four samples of each material. The film thicknesses were measured to be in the range of 55 – 75 nm for all samples.

To calculate the molar density of each sample, we used film thickness obtained from ellipsometry and determined the mass of the films using an absorption measurement recorded in the spectral range 300 nm – 480 nm. We first measured the absorbance of a 3 ml reference solution with known mass of the dissolved material which was prepared from a stock solution of higher concentration. The film samples were then each placed in a quartz cuvette (10 mm path length) filled with 3 ml of the same solvent used for spin-coating. We measured the optical density of each dissolved sample, which is depicted in Figure 2. The mass was calculated from (1):

$$m = \frac{a_1}{a_2} m_{ref}, \qquad (1),$$

where m is mass of the film, a_1 is the spectrally integrated absorbance measured for the dissolved film, a_2 is the integrated absorbance measured for the reference sample and m_{ref} is the known mass of the solute in the reference solution. Care was taken to ensure that the film was fully dissolved prior to the absorbance measurement, and after the measurement the substrate was inspected in a fluorescence measurement to validate that the film had been completely removed.
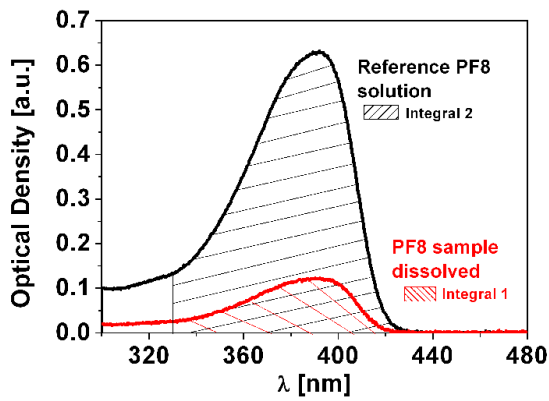

Figure 2. Absorption spectra of the PF8 sample dissolved in 3 ml of solvent and PF8 reference solution. The integral under the absorbance curve was used to calculate the mass of the polymer on the substrate.

The mass density ρ was than calculated from (2):

$$\rho = \frac{m}{V} = \frac{m}{dxy}, \qquad (2),$$

where d is the thickness of the film and x and y are the length and width of the substrate, respectively.

Results and discussion:

Figure 3 shows the absorption and photoluminescence (PL) spectra of polyfluorenes (3a) and truxenes (3b) in the solid state as films. The excitation wavelengths applied were 355 nm for the polyfluorenes and 325 nm for the truxenes. The absorption maxima and main emission peaks for each family are presented in table 2. The absorption in polyfluorenes and truxenes does not change much between the members of each family. We observe a few nanometres spectral shift of the absorption peak towards longer wavelengths with an increase of the side chain length for both families. The PL spectra remain very similar for the truxenes but there is a noticeable red-shift in the PL spectrum of PF12.

Material	AbsMax [nm]	0-0, 0-1 transition [nm]	PLQY
PF 8	386	423, 445	36 %
PF12	392	432, 456	54 %
PF15	395	422, 446	40 %
T3butyl	364	413, 437	63 %
T3hexl	367	412, 435	83 %
T3octyl	368	412, 435	80 %

Table 2. Characteristic peaks of all materials and PLQY

PLQY measurements of thin films were performed using an excitation wavelength of 325 nm for truxenes and 355 nm for polyfluorenes. The solid-state PLQYs were measured in a nitrogen atmosphere and the results are presented in Table 2. The uncertainty of the PLQY measurement is ± 2%.
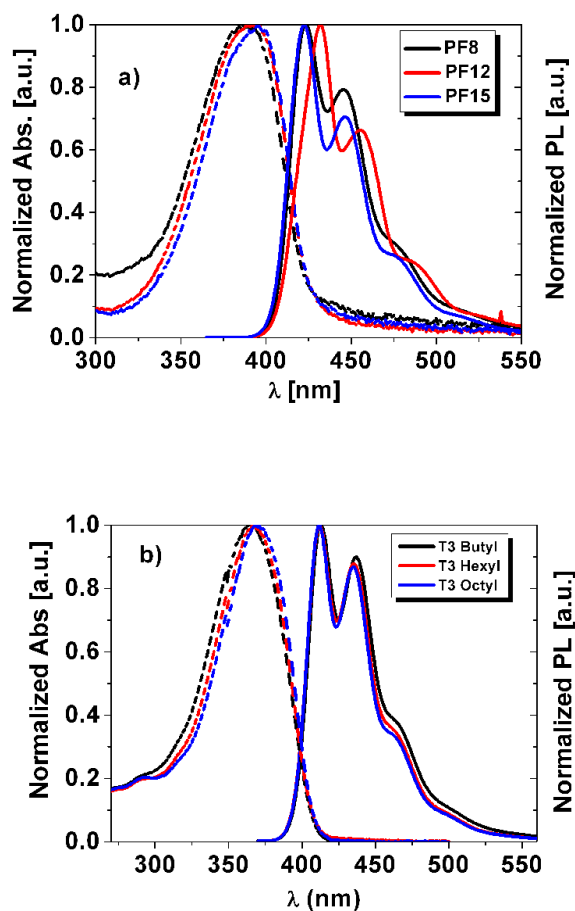
Figure 3 Absorption (dashed line) and fluorescence (solid line) spectra of: a) polyfluorenes, b) truxenes

The ellipsometry data was fitted with an isotropic model to determine film thickness. This choice of model is reasonable as truxene molecules have previously been reported to arrange with random orientations [22], while polymers with low molecular weight also tend towards an isotropic molecular arrangement as shown by Koynov *et al.* [30]. For the particular polymers in this study we also tried an anisotropic model and we found the best fitting was for the isotropic model. The isotropic assumption for polymers is further supported by figure 3a as we cannot see any characteristic features of a crystalline β-phase in the spectra of the polyfluorenes, meaning that our polymer samples were in the glassy α-phase. The fitting

mean squared error (MSE) values for all materials were in the range 0.62 – 1.20 indicating that the model fits very well to the obtained data. The measured film thicknesses for polyfluorenes were in the range 60 – 75 nm and 55 – 60 nm for truxenes.
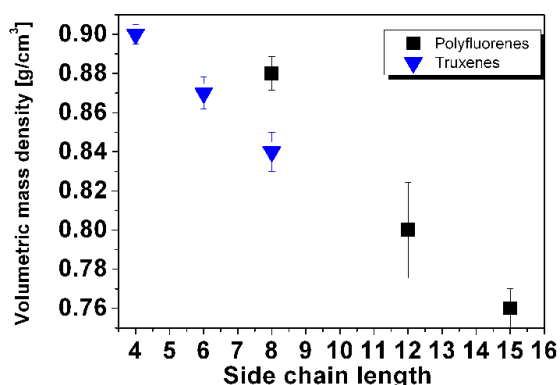

Figure 4. Density of organic materials *vs* the number of carbon atoms in their alkyl side chains.

Figure 4 presents the film density dependence on the side chain length of the polymer or truxene molecules in this study. The density of PF8 is (0.88 ± 0.04) g/cm^3, and of T3 butyl is (0.90 ± 0.04) g/cm^3. For both polyfluorenes and truxenes, the density decreases with an increase of the side chain length. The rate of change in density with side chain length is approximately the same for both sets of materials. For octyl side chains we find that the density is lower for the star-shaped molecules (T3 octyl) than for the polymer (PF8). The lower density of the truxene could arise from its greater rigidity and the star-shape motif inhibiting dense packing. Using the molecular weight and density of the material, we calculated the average spacing of the truxene molecules, as shown in Table 3. From these results we estimate that an increase of the side chain length by two carbon atoms causes approximately an 8% increase in average spacing of the truxene cores.

Material	Density [g/cm^3]	Volume / Molecule	Mean spacing

		[nm³]	(1D) [nm]
T3 butyl	0.90	5.84	1.8
T3 hexyl	0.87	7.33	1.94
T3 octyl	0.84	8.92	2.07

Table 3. Average molecular volume and spacing for the truxene molecules

We repeated the measurement for the organic semiconductor 4,4'-N,N'-dicarbazole-biphenyl (CBP), for which the film density was previously reported [20]. The density of our spin-coated CBP film was found to be (1.08 ± 0.04) g/cm³, whereas the Lai group has reported that the density of CBP for an evaporated film was (1.18 ± 0.02) g/cm³. The difference between the two values could be explained by the different methods of film fabrication. In the case of the slow process of evaporation molecules have much more time for closer packing than for the faster process of spin-coating. Closer packing of molecules will give a higher density of the film. This result is consistent with higher refractive index data measured for evaporated films [31,32].

We have also evaluated the density based on neutron reflectivity results for poly[9,9'-(2-d_{17} – ethylhexyl)fluorene] (PF26) [33]. The scattering length density (SLD) is defined as:

$$SLD = \frac{\rho N_A \sum_i b_i}{M}, \quad (3)$$

where ρ is film density, N_A- Avogadro number, b_i is the coherent scattering length of all nuclei and M is the molecular weight of the repeating unit. After simple rearrangement of equation (3), we can calculate the film density. The SLD reported for PF26 at room temperature was $5.0 \pm 0.1 \times 10^{-6}$ Å^{-2} and using the coherent scattering lengths: $b_C = 6.65$ fm, $b_H = -3.74$ fm and $b_D = 6.67$ fm for carbon, hydrogen and deuterium, respectively, we obtain a

PF26 film density of 0.88 g/cm^3. As the PF26 molecular structure is very similar to the PF8 chemical structure, we expect that they would have similar film density.
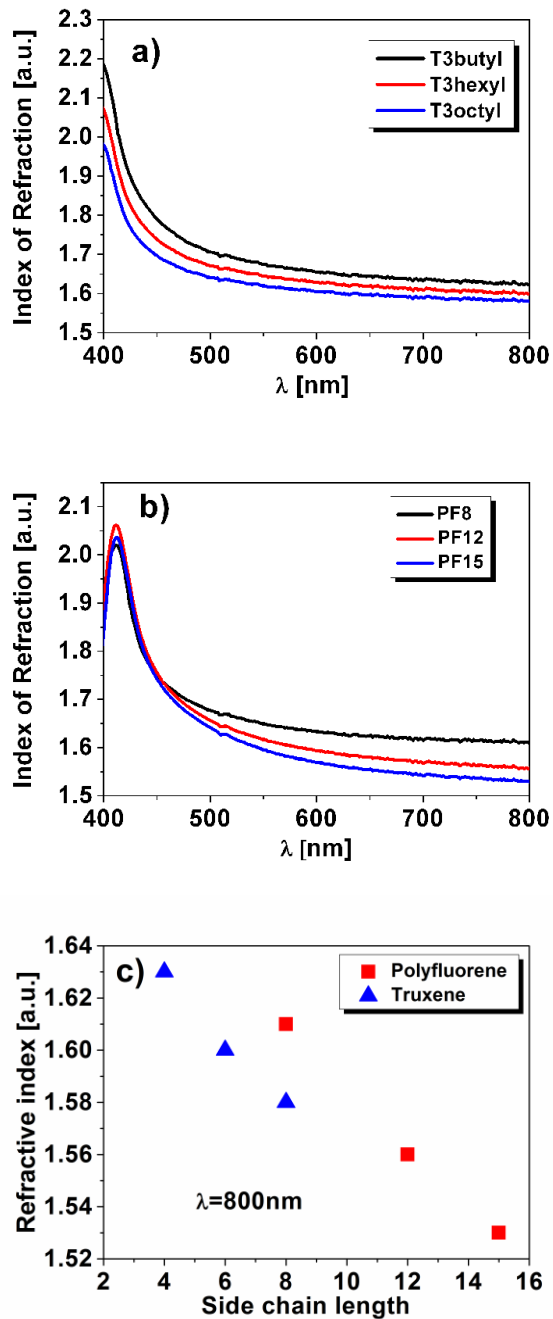

Figure 5 Ellispometry data in the region 400 – 800 nm showing a) the refractive index n for truxenes; b) the refractive index n for polyfluorenes; c) the refractive index dependence on side chain length for truxene molecules and polyfluorenes at 800 nm

From the ellipsometry data we also extracted the wavelength dependence of the refractive index, n, of each material, as shown in Figure 5. The refractive indices of the T3 butyl, T3 hexyl and T3 octyl reduce systematically with increasing side chain length across the full spectra 400 – 800 nm (5a). The polyfluorenes (5b) show the same trend for longer wavelengths (transparent range). In the visible range, however, the PF8 refractive index curve crosses over the other curves. This crossing close to the absorption resonance may be related to the broader, weaker absorption of the PF8, compared with the other two polymers.

Figure 5c compares the refractive indices for both families at 800 nm, far from the absorption. The refractive index shows the same trend as the density in Figure 4, the molecules with shorter side chains having a higher refractive index in the transparent range.

Conclusion

We have presented a detailed investigation of the effect alkyl side chain on the molecular density and refractive index of polyfluorenes and oligofluorene truxenes. We have used an improved solution absorbance method to determine densities of films spin-coated from small molecules and polymers. We observe that the densities of both families decrease with increasing length of alkyl sides chains, and find that their refractive indices correlate with variations in density.

Corresponding Author

Dr Graham Turnbull gat@st-andrews.ac.uk

Present Addresses

† Department of Physics, University of York, Heslington, York, YO10 5DD, UK

References:

(1) Shaheen S.E.; Brabec C.J.; Sariciftci N.S.; Padinger F.; Fromherz T.; Hummele J.C. 2.5% efficient organic plastic solar cells. *Appl. Phys. Lett.* **2001**, *78*, 841–843.

(2) Scharber M.C.; Sariciftci N.S., Efficiency of bulk-heterojunction organic solar cells. *Prog. Polym. Sci.* **2013**, *38*, 1929-1940.

(3) Zhang S.; Turnbull G.A.; Samuel I. D.W. Highly efficient solution-processable europium-complex based organic light-emitting diodes. *Org. Elect.* **2012**, *13*, 3091–3096.

(4) Zhang S.; Turnbull G. A.; and Samuel I.D.W. Enhancing the emission directionality of organic light-emitting diodes by using photonic microstructures. *Appl. Phys. Lett.* **2013**, *103,* 213302.

(5) Muccini M. A bright future for organic field-effect transistors. *Nat. Mater.* **2006**, *5*, 605 – 613.

(6) Turnbull G.A. ; Andrew P.; Jory M.J.; Barnes W.L.; Samuel I.D.W. Emission characteristics and photonic band structure of microstructured polymer lasers. *Synth. Met.* **2002**, *127* , 45-48.

(7) Vasdekis A.E.; Tsiminis G.; Ribierre J.C.; O`Faolain L.; Krauss T.F.; Turnbull G.A. and Samuel I.D.W. Diode pumped distributed Bragg reflector lasers based on a dye-to-polymer energy transfer blend. *Opt. Exp.* **2006**, *14*, 9211.

(8) Yang Y.; Samuel I.D.W. and Turnbull G.A. Sensitive Explosive Vapor Detection with Polyfluorene Lasers. *Adv. Mater.* **2009**, *21* , 3205–3209.

(9) Yang J.S. and Swager T.M. Fluorescent Porous Polymer Films as TNT Chemosensors: Electronic and Structural Effects *J. Am. Chem. Soc.* **1998**, *120,* 11864–11873.

(10) Rose A.; Zhu Z.G.; Madigan C.F.; Swager T.M.; Bulovic V. Sensitivity gains in chemosensing by lasing action in organic polymers. *Nat.* 2005, *434*, 876- 879.

(11) Haughey A.M.; Guilhabert B.; Kanibolotsky A.L.; Skabara P.J.; Dawson M.D.; Burley G.A.; Laurand N.,An oligofluorene truxene based distributed feedback laser for biosensing

applications. *Bios. Bioel.* **2014**, *54*, 679-686.

(12) Schwartz B. J. Conjugated polymers as molecular materials: how chain conformation and film morphology influence energy transfer and interchain interactions. *Annu. Rev. Phys. Chem.* **2003**, *54*, 141.

(13) Frampton M.J.; Magennis S.W.; Pillow J.N.G.; Burn P.L. and Samuel I.D.W. The effect of intermolecular interaction on the electro-optical properties on porphyrin dendrimers with conjugated dendrons. *J. Mater.Chem.* **2003**, 13, 235-242.

(14) Kline R.J. and McGehee M.D. Morphology and charge transport in Conjugated Polymers. *J. of Mech. Sci. C Pol. Rev.* **2006**, *46*, 27-45.

(15) Lupton J. M.; Samuel I. D. W.; Beavington R.; Frampton M. J.; Burn P. L. and Bässler H., Control of mobility in molecular organic semiconductors by dendrimer generation. *Phys. Rev. B* **2001**, *63*, 155206.

(16) Hedley G.J.; Ward A.J.; Alekseev A.; Howells C.T.; Martins E.R.; Serano L.A.; Cooke G.; Ruseckas A. and Samuel I.D.W. Determining the optimum morphology in high-performance polymer-fullerene organic photovoltaic cells. *Nat. Comm.* **2013**, 4, 2867.

(17) Waseda A.; Fujii K. and Taketoshi N. Density measurement of Thin-Film by a Pressure-of-Flotation Method. *IEEE Trans. on Instrument. and Measur.* **2005**, *54*, 882-885.

(18) Schalchil A.; Benattar J.J. and Licoppe C. Accurate Measurements of the Density of Thin Silica Films. *Europhys. Lett* **1994**, *26,* 271-276.

(19) Chen S.H.; Chou H.L.; Chen S.A. and Su A.C. Molecular Packing in Crystalline Poly(9,9-di-n-octyl-2,7-fluorene). *Macromolecules* **2004**, *37*, 6833-6838.

(20) Xiang H.F.; Xu Z.X.; Roy V.A.L.; Che C.M. and Lai P.T. Method of measurement of the density for thin films of small organic molecules. *Rev. Sci. Instrum.* **2007**, *78*, 034104.

(21) Heliotis G.; Xia R.; Bradley D.D.C.; Turnbull G.A.; Samuel I. D. W.; Andrew P. and Barnes W.L. Blue, surface-emitting, distributed feedback polyfluorene lasers. *Appl. Phys. Lett*. **2003**, *83*, 2118-2120.

(22) Wang Y.; Tsiminis G.; Yang Y.; Ruseckas A.; Kanibolotsky A.L.; Perepichka I.F.; Skabara P.J.; Turnbull G.A.; Samuel I.D.W. Broadly tunable deep blue laser based on a star-shaped oligofluorene truxene**.** *Synth.Met.* **2010**, *160,* 1397-1400.

(23) Kanibolotsky A.L.; Berridge R.;. Skabara P.J.; Perepichka I.F.; Bradley D.D.C.; Koeberg M. Synthesis and Properties of Monodisperse Oligofluorene-Functionalized Truxenes: Highly Fluorescent Star-Shaped Architectures*J. Am. Chem. Soc.* **2004**, 126,13695-13702.

(24) Lai W.Y.; Xia R.; He Q.Y.; Levermore P.A.; Huang W. and Bradley D.D.C. Enhanced Solid-State Luminescence and Low-Threshold Lasing from Starburst Macromolecular Materials. *Adv. Mater.* **2009**, *21*, 355360.

(25) Grell M.; Knoll W.; Lupo D.; Meisel A.; Miteva T.; Neher D.; Nothofer H.G.; Scherf U.; Yasuda A. Blue Polarized Electroluminescence from a Liquid Crystalline Polyfluorene. *Adv. Mater.* **1999**, *11*, 671-675.

(26) Gomulya W.; Constanzo G. D.; Figueiredo de Carvalho E. J.; Bisri S. Z., Derenskyi V.; Fritsch M.; Fröhlich N.; Allard S.; Gordiichuk P.; Herrmann A.; et al. Semiconducting Single-Walled Carbon Nanotubes on Demand by Polymer Wrapping. *Adv. Mater.* **2013**, *25*, 2948.

(27) Samanta S. K.; Fritsch M.; Scherf U.; Gomulya W.; Bisri S. Z.; Loi M. A. Conjugated polymer-assisted dispersion of single-wall carbon nanotubes: the power of polymer wrapping. *Acc. Chem. Res*. **2014**, *47*, 2446.

(28) Nehls B. S.; Asawapirom U.; Füldner S.; Preis E.; Farrell T.; Scherf U. Semiconducting Polymers via Microwave-Assisted Suzuki and Stille Cross-Coupling Reactions. *Adv. Funct. Mater.* **2004**, *14*, 352-356

(29) Greenham N.C.; Samuel I.D.W.; Hayes G.R.; Phillips R.T.; Kessener Y.A.R.R.; Moratti S.C.; Holmes A.B.; Friend R.H. Measurement of absolute photoluminescence quantum efficiencies in conjugated polymers. *Chem. Phys. Lett.* **1995**, *241*, 89-96.

(30) Koynov K.; Bahtiar A.; Ahn T.; Cordeiro R.M.; Hörhold H.H. and Bubeck C. Molecular Weight Dependence of Chain Orientation and Optical Constants of Thin Films of the Conjugated Polymer MEH-PPV. *Macromolecules* **2006**, *39*, 8692-8698.

(31) Kim H.; Byun Y.; Das R.R.; Choi B.-K.; and Ahn P.-S. Small molecule based and solution processed highly efficient red electrophosphorescent organic light emitting devices. *Appl. Phys. Let.* **2007**, *91*, 093512.

(32) Lee T.-W.; Noh T.; Shin H.-W.; Kwon O.; Park J.-J.; Choi B.-K.; Kim M.-S.; Shin D.W.; Kim Y.-R. Characteristics of Solution-Processed Small-Molecule Organic Films and Light-Emitting Diodes Compared with their Vacuum-Deposited Counterparts. *Adv. Funct. Mater.* **2009**, *19*, 1625-1630.

(33) Mitchell W.J.; Burn P. L.; Thomas R.K.; Fragneto G.; Markham J.P. J. and Samuel I. D. W. Relating the physical structure and optical properties of conjugated polymers using neutron reflectivity in combination with photoluminescence spectroscopy. *J. Appl. Phys.* **2004**, 95, 2391.

Table of Contents Image: